IN THE UNITED STATES PATENT AND TRADEMARK OFFICE

Application No.	:10/659,090	Confirmation No.:2724
Applicant	:Christopher J. Nagel	
Filed	:September 10, 2003	
TC/A.U.	:1751	
Examiner	:Mark T. Kopec	
Docket No.	:2751.2001 US2	
Title:	COMPOSITION OF MATTER TAILORING: SYSTEM I	

CERTIFICATE OF MAILING OR TRANSMISSION
I hereby certify that this correspondence is being deposited with the United States Postal Service with sufficient postage as First Class Mail in an envelope addressed to Commissioner for Patents, P.O. Box 1450, Alexandria, VA 22313-1450, or is being facsimile transmitted to the United States Patent and Trademark Office on:

August 16, 2006 [signature]
Date Signature

Lorraine Miller Doyle
Typed or printed name of person signing certificate

Commissioner for Patents
P.O. Box 1450
Alexandria, VA 22313-1450

DECLARATION UNDER 37 CFR 1.132

Sir:

I, Christopher J. Nagel, of 28 Highland Circle, Wayland MA 01778, am the sole inventor of the above identified application. I am the sole inventor of the above identified patent application.

I am attaching a detailed description of each of the analytical techniques described in this declaration and in my Declaration under 37 CFR 1.132 filed on March 23, 2006. These techniques were performed by third party companies to confirm the change in matter achieved through tailoring (Exhibit 1). GDMS was obtained from SHIVA Technologies of Syracuse, New York; XRF was obtained from the University of Western Ontario, London, Ontario; PIXE was obtained from Elemental Analysis Incorporated,

Lexington, Kentucky; and GDOES was obtained from Twin Analytical of Independence, Ohio.

I have been asked to clarify the process of manufacture for the copper samples described in my earlier Declaration under 37 CFR 1.132. The copper sample in the declaration, as are the samples described herein, refer to the ingot number of the sample. Copper 14-00-01 corresponds to Example 11 of the present application.

As explained previously, third party data confirms that the manufactured copper ingot contains a different elemental signature from naturally occurring copper (Exhibit 3) and my earlier Declaration. To show that the process of the present invention is not unique to copper, I am also attaching third party data for the following elements: aluminum (Exhibit 4), silicon (Exhibit 5), iron (Exhibit 6), nickel (Exhibit 7), and cobalt (Exhibit 8) together with their respective experimental procedures. Please note that the aluminum example is not described in the current application, but rather in my copending application number 11/063,694. The aluminum ingot was produced in accordance with the methods described in these patent applications. The third party data confirmed the unique electronic characteristic of each tailored system. Please note that the spreadsheets in Exhibits 3-8 include GD-MS analyses of each of the starting materials. Further Exhibits 3-8 include the manufacturer's specifications of the starting materials for each system.

I have been asked to provide visual support for the teachings in the specification of the magnetic properties of the tailored copper produced by the present process. I am attaching six photographs of the tailored copper ingot 14-00-01, corresponding to Example 11 of the present specification, (Exhibit 2). I personally observed the magnetic properties described in the slides of Exhibit 2.

I have been asked to analyze a "magnetic copper" sample obtained from Goodfellow Cambridge Limited. As shown in Exhibit 2, the photographs reveal the presence of iron impregnated in copper. In my opinion, the substantial presence of iron creates the magnetic property. Therefore, it is my opinion that the material is not copper substantially free of other metals.

I hereby declare that all statements made herein of my own knowledge are true and that all statements made on information and belief are believed to be true; and further

that these statements were made with the knowledge that willful false statements and the like so made are punishable by fine or imprisonment, or both, under Section 1001 of Title 18 of the United States Code and that such willful false statements may jeopardize the validity of the application or any patent issued thereon.

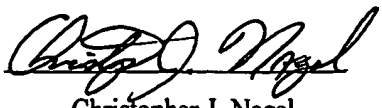

Christopher J. Nagel

Natural Silicon Manufacturer's Specification

ATLANTIC EQUIPMENT ENGINEERS
HIGH PURITY METALS AND COMPOUNDS

13 Foster St., P.O. Box 181, Bergenfield, NJ 07621
TEL: (800) 486-2436 • FAX: (201) 387-0291

a Division of MICRON METALS, Inc.

Certificate of Analysis

SOLD TO:	QUANTUM CATALYTICS
CUSTOMER PO:	20429
SHIP DATE:	30 MAR 01
CATALOG NUMBER	[redacted]
LOT #:	[redacted]
ITEM NAME:	SILICON METAL POWDER
CAS NUMBER:	7440-21-3
DOCUMENT:	103215
QUANTITY:	26 LBS

CHEMICAL ANALYSIS

SILICON	99.99+%

SCREEN ANALYSIS

100% +100 mesh

The above analysis is carried out as part of our internal quality control testing and is based upon our analysis methods

We do not assume any warranty, liability, or risk based on such findings. Our quality is warranted within the scope of our general sales conditions.

Very Truly Yours,

M. Gerald, QA

EXPERIMENTAL PROCEDURE FOR SILICON 15-01-01

EXAMPLE 7

A cylindrical alumina-based crucible (99.68% Al_2O_3, 0.07% SiO_2, 0.08% Fe_2O_3, 0.04% CaO, 0.12% Na_2O_3; 4.5" O.D. x 3.75" I.D. x 10" depth) of a 100 pound induction furnace reactor (Inductotherm) fitted with a 75-30R Powertrak power supply was charged with 700 g Silicon (100.00% purity), through its charging port. The reactor was fitted with a graphite cap and a ceramic liner (i.e., the crucible, from Engineering Ceramics). During the entire procedure, a slight positive pressure of nitrogen (~0.5 psi) was maintained in the reactor using a continuous backspace purge. The reactor was heated to the metal charge liquidus point plus 300°F, at a rate no greater than 300°F/hour as limited by the integrity of the crucible. The induction furnace operated in the frequency range of 0 kHZ to 3000kHz, with frequency determined by a temperature-controlled feedback loop implementing an Omega Model CN 300 temperature controller. Upon reaching 2800°F, the reactor was charged with an additional 400 g Silicon again using a rate no greater than 300°F/hour.

The temperature was again increased to 2900°F again using a rate no greater than 300°F/hour. When this temperature was reached, graphite saturation assemblies (3/8" OD, 36" long high purity (5 ppm impurities) graphite rods) were inserted to the bottom of the Silicon charge through ports located in the top plate. The Silicon was held at 2900°F for 4 hours. Every 30 minutes during the hold period, an attempt was made to lower the graphite saturation assemblies as dissolution occurred. As the Silicon became saturated with carbon, the graphite saturation assemblies were consumed. After the 4 hour hold period was complete, the graphite saturation assemblies were removed.

The reactor temperature was increased to 2976°F over 7 minutes. The temperature was then varied between 2920°F and 2976°F for 15 cycles. Each cycle consisted of lowering the temperature continuously over 7 minutes and raising the temperature continuously over 7 minutes. After the 15 cycles were completed, a gas addition lance was lowered into the molten metal to a position approximately 2" from the bottom of the reactor and a 0.15 L/min flow of argon was begun. The temperature of the Silicon was varied over another 5 cycles between 2920°F and 2976°F.

After the fifth cycle, the reactor temperature was lowered to 2900°F over a 10 minute period with continued argon addition. The graphite saturation assemblies were reinstalled in the Silicon and remained there for 1 hour. The graphite saturation assemblies were removed.

The reactor temperature was lowered to 2895°F over 5 minutes. The reactor was held at this temperature for 5 minutes with continued argon addition. The temperature was then varied between 2886°F and 2895°F over 20 cycles. Each cycle consisted of lowering the temperature continuously over 9 minutes and raising the temperature continuously over 9 minutes. The argon addition ceased after completion of the 20 cycles.

The reactor temperature was lowered to 2873°F over 5 minutes. The temperature was varied between 2868°F and 2873°F over 4 ½ cycles. Each cycle consisted of lowering the temperature continuously over 5 minutes and raising the temperature continuously over 3 minutes. In addition, while raising the temperature, a 0.15 L/min flow of argon was added, and while lowering the temperature, a 0.15 L/min flow of nitrogen was added.

The reactor temperature was lowered to 2863°F over 5 minutes. The temperature was varied between 2811°F and 2863°F for 15.5 cycles. Each cycle consisted of lowering the temperature continuously over 15 minutes and raising the temperature continuously over 15 minutes. In addition, while raising the temperature, a 0.15 L/min flow of argon was added, and while lowering the temperature, a 0.15 L/min flow of nitrogen was added. All gas addition, except for the purge of nitrogen ceased after the 15.5 cycles were completed.

The temperature was varied between 2833°F and 2811°F for one cycle. The cycle consisted of raising the temperature continuously over 15 minutes and lowering the temperature continuously over 15 minutes. The gas addition lance was removed .

The reactor temperature was slowly cooled by lowering the induction furnace power to 1 kW or less s the ingot cooled. After solidification, the Silicon was cooled to approximately ambient temperature in water.

ANALYTICAL PROTOCOLS

XRF, grain size, magnetism, and chemical reactivity measurements were carried out by the procedures described in Example 1.

ANALYTICAL RESULTS

An x-ray fluorescence analysis of the silicon sample is provided in Figures 45A and 45B, with the K_α and L_α peaks of a silicon control standard shown for reference.

An x-ray fluorescence analysis of the silicon sample is provided in Figure 46A, with the K_α peak of an aluminum control standard shown for reference.

An x-ray fluorescence analysis of the silicon sample is provided in Figure 46B, with the K_α peak of a titanium control standard shown for reference.

An x-ray fluorescence analysis of the silicon sample is provided in Figure 47A, with the K_α peak of a sulfur control standard shown for reference.

An x-ray fluorescence analysis of the silicon sample is provided in Figure 47B, with the K_α peak of a chlorine (from potassium chloride) control standard shown for reference.

An x-ray fluorescence analysis of the silicon sample is provided in Figure 48A, with the K_α peak of a gallium control standard shown for reference.

An x-ray fluorescence analysis of the silicon sample is provided in Figure 48B, with the K_α peak of a potassium control standard shown for reference.

Summary data showing the apparent elemental composition of the product of Example 7 is shown in Tables 24-27, as was measured by an XRF analysis using a Uniquant software package. The apparent elemental composition of the product varies by position, which is indicated in each table.

No unexpected magnetic activity or chemical reactivity were recorded for the ingot. The manufactured silicon system did appear shiny on its axial (top) face and dull on is radial (side) face. The ingot retained minimal refractory upon removal from the reactor.

Natural Copper Manufacturer's Specification

Hickman, Williams & Company

MATERIALS FOR THE METALS INDUSTRY
CHICAGO • CINCINNATI • CLEVELAND
DETROIT • PHILADELPHIA • PITTSBURGH
CAMBRIDGE, ONTARIO

CERTIFICATE OF ANALYSIS

TO: Quantum Catalytics DATE: 11/10/99

LOT # 120 PO # 10190

MATERIAL: *COPPER CHOPS* WEIGHT: 5000 lbs.

TIN	.0014	COPPER	99.98
IRON	.0037	SELENIUM	ND
ANTIMONY	ND	ARSENIC	ND
SULFUR	.0007	BISMUTH	ND
CADMIUM	ND	COBALT	ND
ZINC	ND	NICKEL	.0008
SILVER	ND	LEAD	.0038
PHOSPHOROUS	ND	MANGANESE	ND

*less than

Certified by: *Russell L. Etherington*

EXPERIMENTAL PROCEDURE FOR COPPER 14-00-01
(EXAMPLE 11)

A cylindrical alumina-based crucible (89.07% Al_2O_3, 10.37% SiO_2, 0.16% TiO_2, 0.15% Fe_2O_3, 0.03% CaO, 0.01% MgO, 0.02% Na_2O_3, 0.02% K_2O; 9" O.D. x 7.75" I.D. x 14" depth) of a 100 pound induction furnace reactor supplied by Inductotherm, fitted with a 75-30R Powertrak power supply, was charged with 100 pounds copper (99.98% purity) through its charging port. During the entire procedure, a slight positive pressure of nitrogen (~0.5 psi) was maintained in the reactor using a continuous backspace purge. The reactor was heated to the metal charge liquidus point plus 300°F, at a rate no greater than 300°F/hour, as limited by the integrity of the crucible. The induction furnace operated in the frequence range of 0 kHz to 3000 kHz, with frequency determined by a temperature-controlled feedback loop implementing an Omega Model CN300 temperature controller.

The temperature was again increased to 2462°F again using a rate no greater than 300°F/hour. When this temperature was reached, graphite saturation assemblies (3/8" OD, 36" long high purity (<5 ppm impurities) graphite rods) were inserted to the bottom of the copper charge through ports located in the top plate. The copper was held at 2462°F for 4 hours. Every 30 minutes during the hold period, an attempt was made to lower the graphite saturation assemblies as dissolution occurred. As the copper became saturated with carbon, the graphite saturation assemblies were consumed. After the 4 hour hold period was complete, the graphite saturation assemblies were removed.

The reactor temperature was increased to 2480°F over 7 minutes. The temperature was then varied between 2480°F and 2530°F for 15 cycles. Each cycle consisted of raising the temperature continuously over 7 minutes and lowering the temperature continuously over 7 minutes. After the 15 cycles were completed, a gas addition lance was lowered into the molten metal to a position approximately 2" from the bottom of the reactor and a 1.5 L/min flow of argon was begun. The temperature of the copper was varied over another 5 cycles between 2480°F and 2530°F.

After the fifth cycle, the reactor temperature was lowered to 2462°F over a 10 minute period with continued argon addition. The graphite saturation assemblies were

reinstalled in the copper and remained there for 1 hour. The graphite saturation assemblies were removed.

The reactor temperature was lowered to 2459°F over 5 minutes. The reactor was held at this temperature for 5 minutes with continued argon addition. The temperature was then varied between 2459°F and 2453°F over 20 cycles. Each cycle consisted of lowering the temperature continuously over 9 minutes and raising the temperature continuously over 9 minutes. The argon addition ceased after completion of the 20 cycles.

The reactor temperature was lowered to 2450°F over 5 minutes. The temperature was varied between 2450°F and 2441°F over 4 ½ cycles. Each cycle consisted of lowering the temperature continuously over 5 minutes and raising the temperature continuously over 3 minutes. In addition, while raising the temperature, a 1.5 L/min flow of argon was added, and while lowering the temperature, a 1.5 L/min flow of nitrogen was added.

The reactor temperature was lowered to 2438°F over 5 minutes. The temperature was varied between 2438°F and 2406°F for 15.5 cycles. Each cycle consisted of lowering the temperature continuously over 15 minutes and raising the temperature continuously over 15 minutes. In addition, while raising the temperature, a 1.5 L/min flow of argon was added, and while lowering the temperature, a 1.5 L/min flow of nitrogen was added. All gas addition, except for the purge of nitrogen ceased after the 15.5 cycles were completed.

The temperature was varied between 2406°F and 2419°F for one cycle. The cycle consisted of raising the temperature continuously over 15 minutes and lowering the temperature continuously over 15 minutes. The gas addition lance was removed.

The reactor temperature was rapidly cooled by quenching in water, so that the copper solidified into an ingot.

ANALYTICAL PROTOCOLS

XRF, grain size, magnetism, and chemical reactivity measurements were carried out by the procedures described in Example 1.

ANALYTICAL RESULTS

Summary data showing the apparent elemental composition of the product of Example 11 is shown in Tables 32-33, as was measured by an XRF analysis using a Uniquant software package. The apparent elemental composition of the product varies by position, which is indicated in each table.

Immediately after the method described above was completed, multiple discrete magnetic spots attracted by a 1/8" diameter neodymium iron boron magnet were observed in a sinusoidal pattern. The ingot exhibited point attraction to iron filings at reduced temperatures at or near 77 K. Over days to months, the strength of the magnetic attraction decreased on a fraction of the locations exhibiting magnetic attraction or attraction to iron filings.

Various forms of ligated chlorine (e.g., HCl and MCl, where M is a metal as defined above) readily reacted with the manufactured copper form yielding product distributions distinguishable from natural copper, thereby demonstrating a change in chemical reactivity. This reactivity increased over time.

Extremely large grain sizes (i.e., greater than 1") were observed, which is uncharacteristic and previously unreported in natural copper systems (typically, copper grains sizes are 10-100 μm). Unique changes in coloration were observed with the crossing of grain boundaries; however, the overall coloration mimicked natural copper.

EXHIBIT 1

Analytical Techniques

Analytical Techniques

This document reviews the analytical techniques used to perform the elemental analyses described herein. The descriptions (including lower detection limits, LDLs) are taken primarily from reference and textbooks[1,2,3] and the sources of the individual third-party analytical laboratories that performed the analysis. These sources are referenced for the reader who is interested in a more in-depth description, including schematics. The descriptions below are abbreviated extractions from each of these sources. In addition, Table 1 gives an overview of the analytical protocol followed by the investigators to obtain the submitted data. Table 2 delineates the activation and detection methods used by each method allowing a ready comparison of the similarities and differences of each technique.

Glow Discharge Mass Spectrometry (GD-MS)[4]

Bulk composition analysis (continuous sample consumption) based on the weights of ions sputtered from the sample using a DC plasma. Typical LDLs on the order of parts per billion (ppb, element dependent). Method identical to GD-OES except detection/identification method based on mass, not electronic character.

- *Solid sample is atomized by sputtering in a low-pressure DC plasma*
- *Sputtered atoms are then ionized and extracted into a mass analyzer for separation and detection*
- *Mass to charge ratios are well known allowing identification of elemental species*

Positive ions formed in the Argon plasma glow are accelerated toward the sample. Upon impacting the surface of the sample, neutral particles (predominantly individual atoms) and positive ions are released. The sputtered neutral particles diffuse across the plasma "dark space" and are ionized through interaction with the metastable argon ions of the plasma primarily forming singly charged ions. These singly charged ions are extracted into a mass analyzer for separation and detection. The Mass to Charge ratios are used for elemental species identification.

Glow Discharge Optical Emission Spectrometry (GD-OES)[5]

Quantitative Depth Analysis (near surface 0.05-150 mm) based on the optical emissions (wavelength) of material sputtered from sample surface. Typical LDLs of ~5

---

[1] **Handbook of Instrumental Techniques for Analytical Chemistry**, Frank A. Settle (Ed), Prentice Hall, June 1997.

[2] **Handbook of Analytical Techniques, Vol 1 & 2**; Helmut Günzler, Alex Williams (Eds) John Wiley & Sons, Inc., May 2001

[3] **Practical Handbook of Spectroscopy**, J.W. Robinson (Ed.), CRC Press, Inc., 1991

[4] Shiva Technologies, Inc. Trace Elemental Analysis, Glow discharge Mass Spectrometry Principles, ©2001. http://www.shivatec.com/new/gdmsdesc.php4

[5] Twin Analytical, Glow Discharge Optical Emission Spectrometer, Instrumentation, ©2003-2005. http://www.twinanalytical.com/instruments/GD-OES.php

ppm. Method identical to GD-MS except detection/identification method based on electronic structure.

- *Solid sample is atomized by sputtering in an Ar plasma*
- *Sputtered atoms are then ionized emitting characteristic light emissions*
- *The spectral lines (wavelengths) are indicative of the elemental composition*

Positively charged Ar ions (Ar+) are accelerated, continuously bombarding the sample surface, causing atoms to be ejected. The atoms are excited or ionized in the plasma gas, emitting energy in the form of characteristic light emissions. The light emitted by the sample passes into the spectrometer to photomultiplier tubes that quantify the intensity of the spectral lines (wavelengths). Each element has its own characteristic spectrum and unique wavelength fingerprint (indicative of electron levels) allowing elemental identification.[6,7]

Particle Induced X-ray Emission Spectrometry (PIXE)[8]

Semi-bulk (40 mm penetration depth) analysis based on the emission energies characteristic of electronic orbital shifts. Typical LDLs are on the order of parts per million or higher and are dependent on the element. XRF and PIXE use identical detection methods to identify elemental components of the sample. The sample excitation methods differ in that XRF uses hand X-ray bombardment, while PIXE uses particle (in this case proton) bombardment to induce X-ray emissions.

- *Sample surface is bombarded with protons (H+, 40mm penetration, used in subject technique) or alpha particles (He++, 8 mm)*
- *K-shell electrons are knocked out of innermost electron shell*
- *Electrons from outer shells replace inner shell electrons simultaneously emitting an x-ray*
- *Known x-ray energy emissions allow elemental identification*

Particle Induced X-ray Emission bombards samples with two types of ions, alpha particles (He++) and protons (H+), at high energies. These particles knock out sample electrons from the innermost electron shell, called the K-shell. To fill this vacancy, electrons from the outer shells replace the inner shell electrons with a corresponding emission in energy in the form of an x-ray. Each element has its own characteristic x-ray emission, a unique property, allowing elemental identification. Depth of penetration: 40mm ~ 60mm for copper; 60mm ~ 80mm for aluminum.

X-ray Fluorescence Spectrometry[9]

Semi-bulk composition analysis (1-3 mm penetration depth) based on the emission energies characteristic of electronic orbital shifts. Typical LDLs are approximately 20-

---

[6] **Glow Discharge Optical Emission Spectrometry**, Richard Payling, Delwyn Jones, Arne Bengtson (Eds), John Wiley & Sons, Ltd., 1997.

[7] **Glow Discharge Plasmas in Analytical Spectroscopy**, R. Kenneth Marcus, Jose A. C. Broekaert (Eds.), John Wiley & Sons, Ltd., 2003.

[8] Elemental Analysis Inc., "Proton Induced X-ray Emission"; http://www.elementalanalysis.com/pixe/

[9] Eastern Illinois University, Doug Klarup, Ph.D., Chair Dept. of Chemistry, "X-ray Fluorescence Spectroscopy", http://www.ux1.eiu.edu/~dgklarup/nsfccli/instrumentconcepts/xrf.pdf

50 ppm and are dependent on the individual elements present in the sample matrix. XRF and PIXE use identical detection methods to identify elemental components of the sample. The sample excitation methods differ in that XRF uses X-ray bombardment, while PIXE uses particle (in this case proton) bombardment to induce X-ray emissions.

- *Sample surface is bombarded with x-rays*
- *K-shell electrons are knocked out of innermost electron shell*
- *Electrons from outer shells replace inner shell electrons simultaneously emitting an x-ray*
- *Known x-ray energy emissions allow elemental identification*

A quant of the primary X-ray beam excites atoms of the elements present in the sample removing electrons from the inner-most shell (K-shell). The vacancies are filled with electrons from a higher energy level, the L-shell. As the electron moves to a lower energy shell, a fluorescence quant (emitted x-ray) is created. Its energy is determined by the energetic difference between the L- and the K-shell and is thus characteristic of the element. For these analyses a sequential wavelength dispersive spectrometer (WDS) was used in which specific emission lines are used to determine the presence or absence (and concentrations) of various elements. Each characteristic x-ray line is measured in sequence by the instrument through control of the instrument geometry. The orientation of the detector crystal with respect to the sample and the photon detector is controlled synchronously such that characteristic x-ray lines can be accurately measured. The sequential measurement consists of positioning the diffraction crystal at a given theta (diffraction angle) and the detector at two-theta and counting for a given period. The crystal and detector are then rotated to a different angle for the next characteristic x-ray line.

Neutron Activation Analysis[10]

Bulk composition analysis based on gamma ray emissions induced by neutron bombardment. Typical LDLs range from parts per million to parts per billion and are dependent on the individual elements present in the sample matrix (due to decay interferences). Method is independent of electronic structure and indicative of the structure of the sample's nuclei. "For many elements and applications, NAA offers sensitivities that are superior to those attainable by other methods, on the order of parts per billion or better. In addition, because of its accuracy and reliability, NAA is generally recognized as the "referee method" of choice when new procedures are being developed or when other methods yield results that do not agree"[11].

- *Radioactive isotopes created by neutron bombardment (in nuclear reactor)*
- *>50 elements have stable radioactive isotopes with one neutron more than their stable isotope*

---

[10] General Activation Analysis, Inc., "Neutron Activation Analysis: Method Description", http://generalactivation.com/method.html

[11] Michael D. Glascock, Ph.D. , University of Missouri Research Reactor (MURR); "*An Overview of Neutron Activation Analysis.*" September 12, 2005. http://www.missouri.edu/~glascock/naa_over.htm

- *By detecting the decay of these radioactive nuclei, one measures the concentration of the stable element*

The sample is introduced into the intense radiation field of a nuclear reactor where it is bombarded with neutrons, causing the elements to form radioactive isotopes. The radioactive emissions and radioactive decay paths for each element are well known. Using this information it is possible to study spectra of the emissions of the radioactive sample to determine the concentrations of the sample elements.

Attachments:

Table 1: Analytical Method Overview

Table 2: Analytical Technique Overview by Activation and Detection Mechanism

Table 1: Analytical Method Overview

Technique	XRF	PIXE	GD-OES	GD-MS	NAA
Penetration Depth	1-3 mm	40μm – 80μm	0.05μm – 150μm	~10 mm consumed of 20mm needle	Volumetric
Sample Size	1" x 1" cube	1" x 1" cube	$\frac{1}{8}$" diameter	2mm x 2mm x 20 mm	$\frac{1}{2}$" x 1" cube
Sampled Sides	axial and radial	axial and radial	axial and radial	axial and radial	axial and radial
Sample Configuration	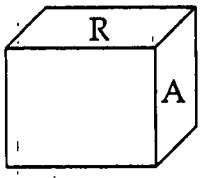	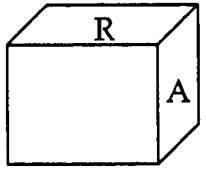	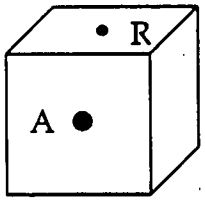	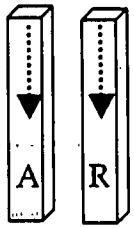	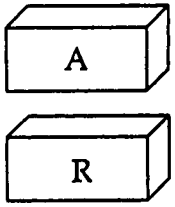
Surface Prep	Polished	Polished	Polished	Polished (ends only)	Saw Cut
Elements Tested	Na – U	Na – U	60	O – U	Na – U
Activation Method	X-ray	H^+	n^+ (Ar^+)	n^+ (Ar^+)	Neutrons
Detection Method	X-ray (wavelength)	X-ray (wavelength)	Photon (wavelength)	Mass	Gamma rays (wavelength)
Typical LDL	50 ppm	Varies by element (OOM ≥ppm)	5 ppm	Varies by element (OOM ppb)	Varies by element (ppm-ppb)

Table 2: Analytical Technique Overview by Activation and Detection Mechanism

Technique	XRF	PIXE	GD-OES	GD-MS	NAA
	X-ray	Proton	Plasma Ionization	Plasma Ionization	Neutron Bombardment
Excited State	Inner Shell e- removal	Inner Shell e- removal	Ionized sputtered individual atoms	Ionized sputtered individual atoms	Isotope creation through nucleus bombardment
Detected Activity	Higher energy electron moves to lower energy shell	Higher energy electron moves to lower energy shell	Ionized atoms emit energy (light) as e- move to lower energy states	Ionized atoms are separated based on weight; most weight in nucleus	Unstable isotopes decay emitting gamma rays
Detection Mechanism	X-ray emitted as e- moves characteristic of element	X-ray emitted as e- moves characteristic of element	Spectral lines characteristic of elements	Mass to charge ratio characteristic of elements	½ life (decay rate) characteristic of element

Electron-based method

Nucleus-based method

EXHIBIT 2

Photographs

Tailored Cu Exhibits Unique Magnetic Behavior

Anisotropic Magnetic Behavior

Equivalent Attraction to North and South Pole

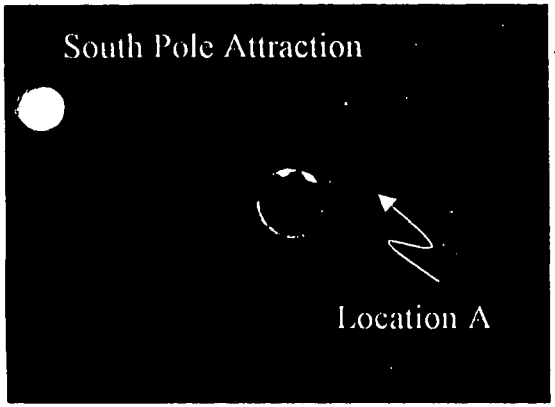

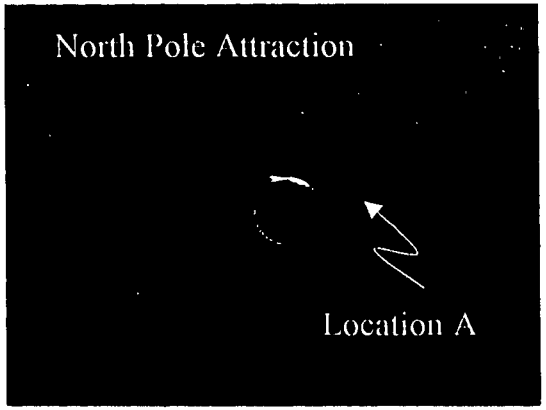

Ingot 14-00-01

Tailored Cu is Magnetic:

- Anisotropic behavior: 1/8" Nd/B/Fe magnet attracted at discrete locations on radial and axial surfaces
- Radial surface exhibited greatest attraction; "Top" axial surface had greater activity than "Bottom" axial surface.
- Magnetic attraction independent of pole.

Elemental Copper Tailored To Reveal Magnetism

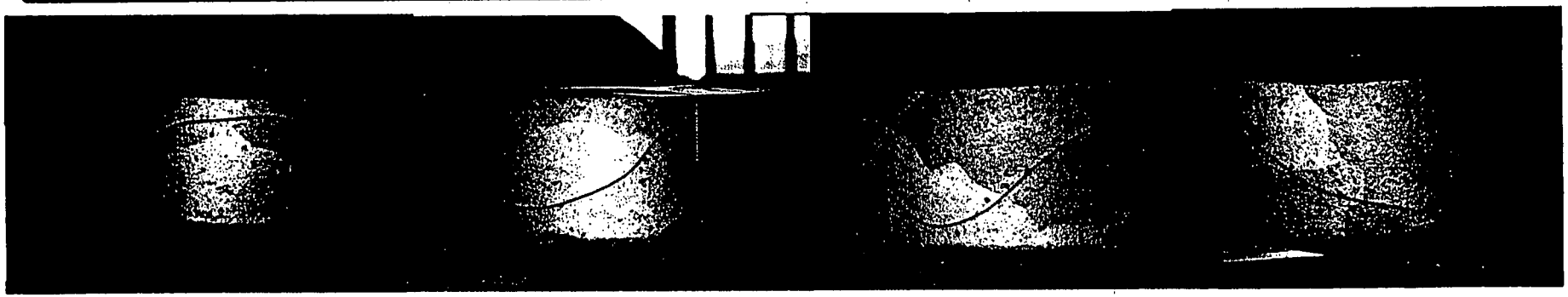

View 1 View 2 View 3 View 4

360° rotation of ingot shown

- Discrete evenly spaced points, forming a sinusoidal pattern, exhibit magnetism.
- Magnetic points exhibit equivalent attraction to the positive and negative poles of a neodymium iron boron magnet independent of temperatures below 373K.
- Magnetic point attraction to iron filings (i.e., ferromagnetism) increases linearly with decreasing temperature (e.g., 298K to 77K).
- The magnetic spots behave in accordance with known magnetic susceptibility relationships as temperature decreases (Feynman).

Magnetic Tailored Copper Attracts Iron

Radial Surface

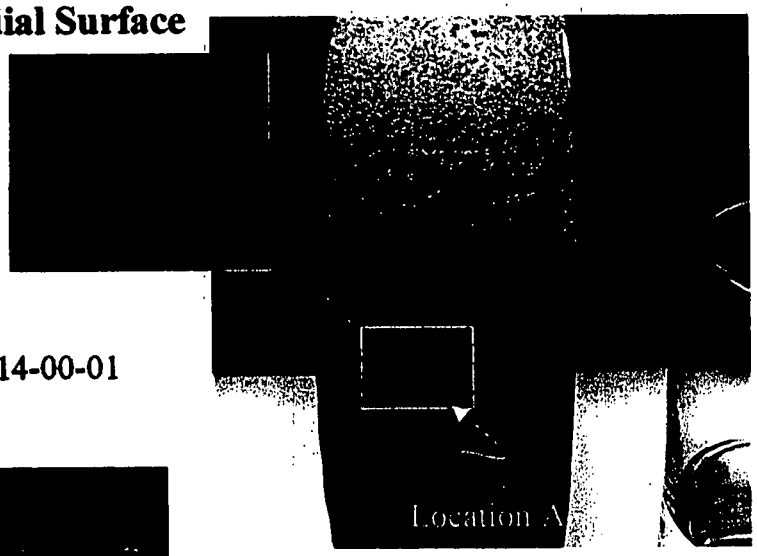

Ingot 14-00-01

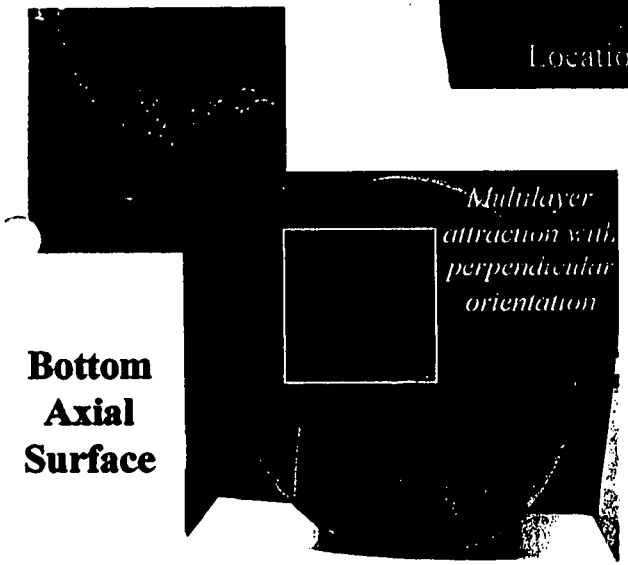

Bottom Axial Surface

- Radial and bottom axial surfaces exhibited greatest activity
  - Multi-layered: strong attraction covering significant distance
  - Oriented: alignment of filings perpendicular to the surface indicative of magnetic origin of attraction
- Top axial surface showed limited regions of anisotropic magnetic behavior

Top Axial Surface

The face of the ingot was covered with Fe filings in a horizontal orientation. The retention of Fe filings in the vertical orientation then showed areas of magnetic activity

Tailored Cu Composite Magnetic Activity

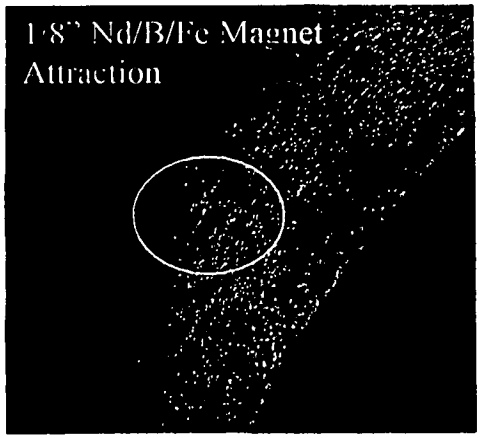

Ingot
14-00-01

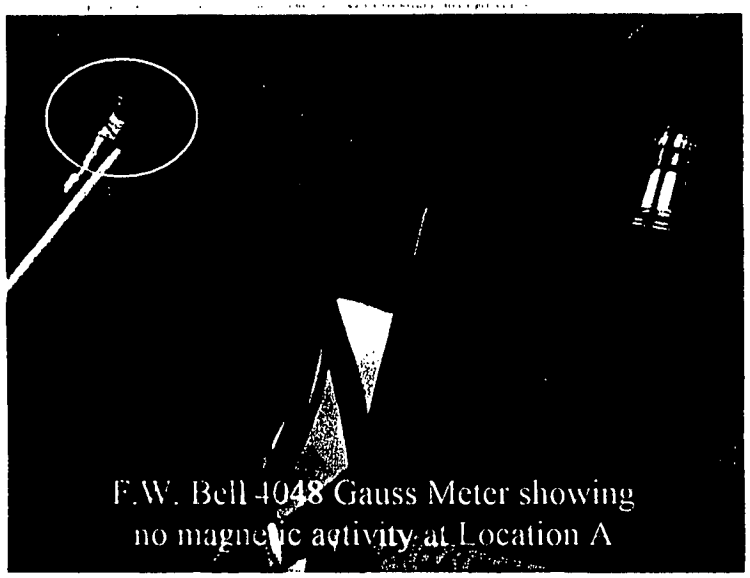

Location A (yellow)

- Attraction to 1/8" Nd/Fe/B magnet
- Attraction to Fe filings
  - Multilayer
  - Perpendicular alignment
- No detectable Gauss reading (0.0)

The magnetic phenomena observed in the tailored copper is inherent to the material and unique to the tailoring/manufacturing process

Recursive Fractal Construction

Points depict attraction to a 1/8" diameter Nd/Fe/B magnet

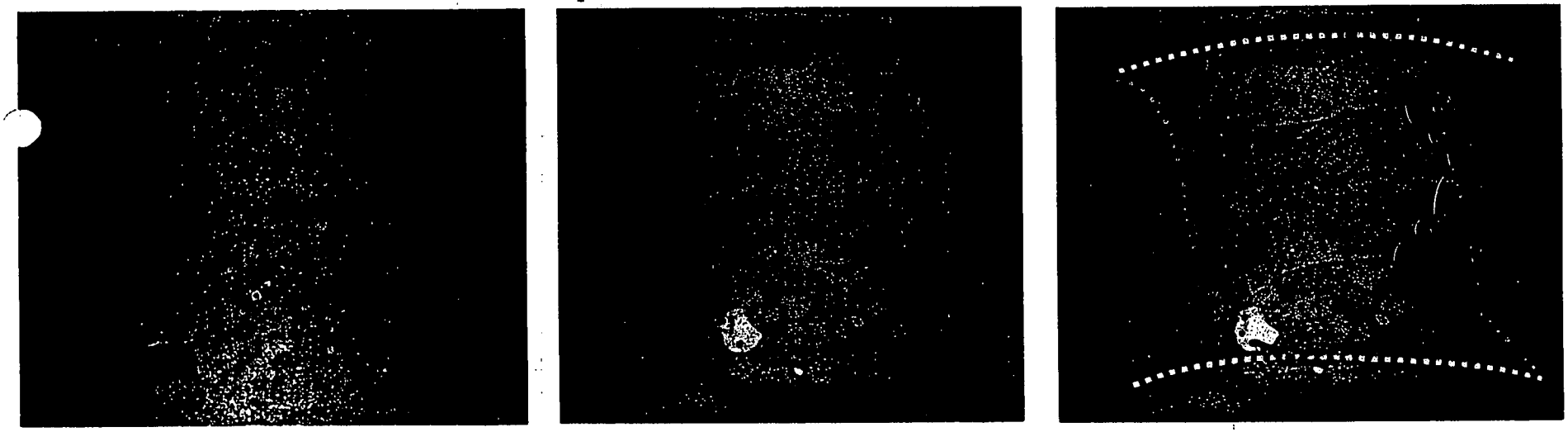

Key:

0^{th} Order Harmonic Scaffolding

1^{st} Order Harmonic Scaffolding

2^{nd} Order Harmonic Scaffolding

n^{th} Order Harmonic Scaffolding

- 1^{st} order harmonic scaffolding exhibits periodicity repeating every 6 inches
- All orders of the harmonic scaffolding are constructed recursively
- The sample contains on order 550 detectable magnetic points

Magnetic Copper: 14-00-01

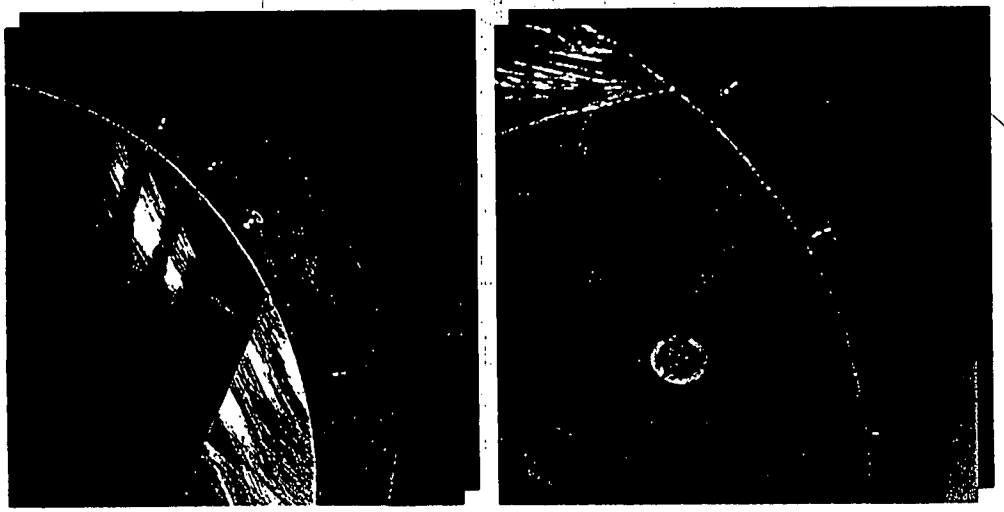

Starting material: ≥ 99.995%$_{wt}$ Cu

- LDLs typically <5 ppm for GD-MS, <20-50 ppm for XRF
- XRF: Multiple elements (X-ray emissions) detected in radial orientation, non-detectable in axial; Fe detected only on axial XRF scan at 53 ppm
- Radial magnetic attraction noted
- High solubility of these elements in a well-mixed molten Cu bath precludes orientation-dependent concentration gradients

Comparison of Third-Party Axial and Radial Elemental Analyses via Weight-Based (GD-MS) Analytical Technique and Electronic-Structure Based (XRF) Analytical Technique (ppm)

	Al	Si	S	Cl	Ti	Fe	Cu	Rh	La	Yb	Re	Ir
GD-MS (Ax)			24				Matrix					
GD-MS (Rad)			24				Matrix					
XRF-UWO (Ax)	1350	6530		112		53	991100	372			126	118
XRF-UWO (Rad)		5640		162	53		993300	315	105	149	155	78

Blanks and all other elements non-detectable to 20 ppm

Goodfellow Cambridge Limited: Magnetic Copper

Magnetic Copper Wire

Composition:	99.96%$_{wt}$ Cu 0.04%$_{wt}$ Fe
Wire Diameter:	0.5mm
Filament Diameter:	0.1 microns
Nos. of Filaments:	16
Length:	5m
Net weight:	9.1 g

Homogeneous alloy
99.96%$_{wt}$ Cu, 0.04%$_{wt}$ Fe

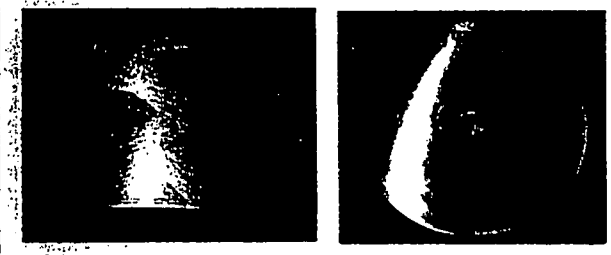

Exhibited no magnetism with Fe/Nd/B supermagnet

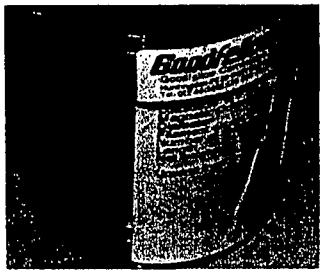

Starting Material

Wire Schematic
(not to scale)

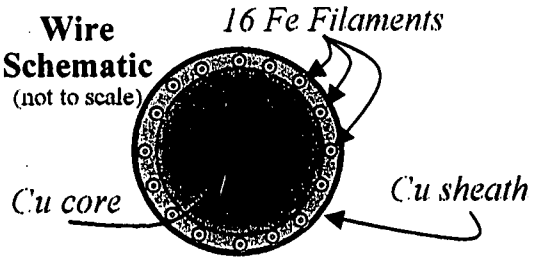

Varying levels of compression

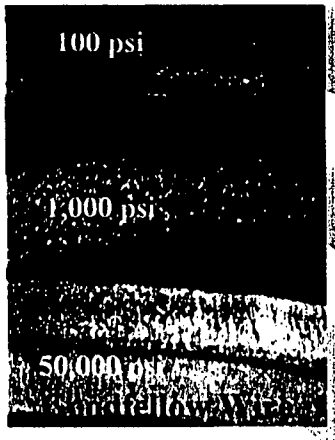

Optical Magnification

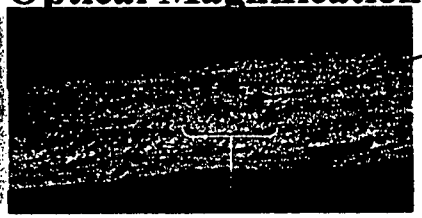

Fe filaments

30x

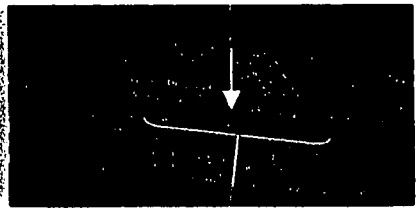

30x

Fe particles after compression

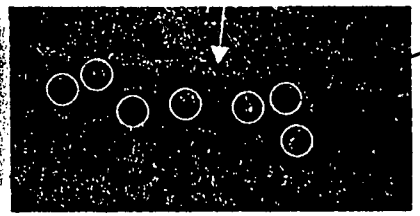

70x

Optical spectroscopy validates that magnetism in Goodfellow "magnetic copper" is caused by iron impregnated in copper

Natural Aluminum Manufacturer's Specification

CERAC™ Incorporated
Quality Manufacturing Since 1964

Certificate of Analysis

Item Number	Description	Lot Number
A-2001	ALUMINUM METAL, Al Typically 99.99% pure 2-12 mm granules	X26242

SPECIFIC ANALYSIS OR PROPERTY

Test For	Found	Theoretical

SPECTROGRAPHIC ANALYSIS

Element	Result (%)	Element	Result (%)	Element	Result (%)
Cr	0.001	Mg	0.001		
Cu	0.002	Si	0.002		

X-RAY DIFFRACTION ANALYSIS

CERAC Incorporated
P.O. Box 1178, Milwaukee, WI 53201
(414) 289-9800 Phone (414) 289-9805 Fax

Brian T Wegner

Brian T Wegner, Q.A. Supervisor — January 7, 2002

OMG AMERICAS

2601 Weck Drive PO Box 12166 Research Triangle Park, NC 27709-2166

LAB ANALYSIS FOR: QUANTUM CATALYTICS
FALL RIVER MA 02720
SHIPPING DOC# 0406898 DATE 07/03/01
PURCHASE ORDER# 905451
CUSTOMER CODE#

GRADE: A-101-A CHIPS/E I MELT STOCK
R05
LOT NUMBER: 04106001 QUANTITY: 100 LB/ 45.36 KG HEAT NUMBER:

CHEMICAL PROPERTIES

Carbon %	.0022
Manganese %	.0012
Nickel %	.0033
Phosphorus %	.0017
Sulfur %	.0024
Silicon %	.0010
Iron %	BALANCE

PHYSICAL PROPERTIES

PERFORMANCE PROPERTIES

SPECIAL PROPERTIES

WE HEREBY CERTIFY THAT THIS MATERIAL WAS MANUFACTURED TO THE REPORTED CHEMISTRY BY OMG AMERICAS ANALYTICAL PROCEDURES FOR A-101-A CHIPS/ E.I. MELT STOCK.

COMMENTS

QS 9000 ISO 9002 ANSI-RAB

APPROVED: John Flynn
TITLE: Lab Manager
LOCATION: Johnstown Pa
(814) 533-7800 ext 802

EXPERIMENTAL PROCEDURE FOR IRON 15-01-02

EXAMPLE 8

A cylindrical alumina-based crucible (99.68% Al_2O_3, 0.07% SiO_2, 0.08% Fe_2O_3, 0.04% CaO, 0.12% Na_2O_3; 4.5" O.D. x 3.75" I.D. x 10" depth) of a 100 pound induction furnace reactor supplied by Inductotherm, fitted with a 75-30R Powertrak power supply was charged with 2000 g Iron (99.98% purity) and 200 g carbon through its charging port. The reactor was fitted with a graphite cap with a ceramic liner (i.e. the crucible, from Engineering Ceramics). During the entire procedure, a slight positive pressure of nitrogen (~0.5 psi) was maintained in the reactor using a continuous backspace purge. The reactor was heated to the metal charge liquidus point plus 300°F, at a rate no greater than 300°F/hour, as limited by the integrity of the crucible. The induction furnace operated in the frequency range of 0 kHz to 3000 kHz, with frequency determined by a temperature-controlled feedback loop implementing an Omega Model CN300 temperature controller. Upon reaching 2800°F, the reactor was charged with an additional 2595 g iron over an hour.

The temperature was again increased to 2850°F again using a rate no greater than 300°F/hour. When this temperature was reached, graphite saturation assemblies (3/8" OD, 36" long high purity (<5 ppm impurities) graphite rods) were inserted to the bottom of the iron charge through ports located in the top plate. The iron was held at 2850°F for 4 hours. Every 30 minutes during the hold period, an attempt was made to lower the graphite saturation assemblies as dissolution occurred. As the iron became saturated with carbon, the graphite saturation assemblies were consumed. After the 4 hour hold period was complete, the graphite saturation assemblies were removed.

The reactor temperature was increased to 3360°F over 7 minutes. The temperature was then varied between 2993°F and 3360°F for 15 cycles. Each cycle consisted of lowering the temperature continuously over 7 minutes and raising the temperature continuously over 7 minutes. After the 15 cycles were completed, a gas addition lance was lowered into the molten metal to a position approximately 2" from the bottom of the reactor and a 0.15 L/min flow of argon was begun. The temperature of the iron was varied over another 5 cycles between 2993°F and 3360°F.

After the fifth cycle, the reactor temperature was lowered to 2850°F over a 10 minute period with continued argon addition. The graphite saturation assemblies were reinstalled in the iron and remained there for 1 hour. The graphite saturation assemblies were removed.

The reactor temperature was lowered to 2819°F over 5 minutes. The reactor was held at this temperature for 5 minutes with continued argon addition. The temperature was then varied between 2622°F and 2818°F over 20 cycles. Each cycle consisted of lowering the temperature continuously over 9 minutes and raising the temperature continuously over 9 minutes. The argon addition ceased after completion of the 20 cycles.

The reactor temperature was lowered to 2724°F over 5 minutes. The temperature was varied between 2622°F and 2724°F over 4 ½ cycles. Each cycle consisted of lowering the temperature continuously over 5 minutes and raising the temperature continuously over 3 minutes. In addition, while raising the temperature, a 0.15 L/min flow of argon was added, and while lowering the temperature, a 0.15 L/min flow of nitrogen was added.

The reactor temperature was lowered to 2586°F over 5 minutes. The temperature was varied between 2133°F and 2586°F for 15.5 cycles. Each cycle consisted of lowering the temperature continuously over 15 minutes and raising the temperature continuously over 15 minutes. In addition, while raising the temperature, a 0.15 L/min flow of argon was added, and while lowering the temperature, a 0.15 L/min flow of nitrogen was added. All gas addition, except for the purge of nitrogen ceased after the 15.5 cycles were completed.

The temperature was varied between 2340°F and 2133°F for one cycle. The cycle consisted of raising the temperature continuously over 15 minutes and lowering the temperature continuously over 15 minutes. The gas addition lance was removed .

The reactor temperature was cooled by lowering the induction furnace power to 1 kW or less as the ingot cooled. After solidification, the iron was cooled to approximately ambient temperature in water.

ANALYTICAL PROTOCOLS

XRF, grain size, magnetism, and chemical reactivity measurements were carried out by the procedures described in Example 1.

ANALYTICAL RESULTS

An x-ray fluorescence analysis of the iron sample is provided in Figures 49A and 49B, with the K_α and L_α peaks of an iron control standard shown for reference.

An x-ray fluorescence analysis of the iron sample is provided in Figure 50A, with the K_α peak of an aluminum control standard shown for reference.

An x-ray fluorescence analysis of the iron sample is provided in Figure 50B, with the K_α peak of an zirconium control standard shown for reference.

An x-ray fluorescence analysis of the iron sample is provided in Figure 51A, with the K_α peak of a sulfur control standard shown for reference.

An x-ray fluorescence analysis of the iron sample is provided in Figure 51B, with the K_α peak of a chlorine (from potassium chloride) control standard shown for reference.

Summary data showing the apparent elemental composition of the product of Example 8 is shown in Tables 28-29, as was measured by an XRF analysis using a Uniquant software package. The apparent elemental composition of the product varies by position, which is indicated in each table.

The manufactured iron exhibited no unexpected magnetic activity. The reactivity relative to that which would be expected from natural iron has not been quantified. The ingot appears glassy or shiny on its axial (top) face and dull on its radial (side) face. The manufactured iron retained a negligible amount of refractory upon removal from the reactor, but cracked upon retrieval. The ingot had no internal voids.

CERAC™ Incorporated
Quality Manufacturing Since 1964

Certificate of Analysis

Item Number	Description	Lot Number
N-1022	NICKEL METAL, Ni Typically 99.9% pure -80, +200 mesh	X0027674

SPECIFIC ANALYSIS OR PROPERTY

Test For	Found	Theoretical

SPECTROGRAPHIC ANALYSIS

Element	Result (%)	Element	Result (%)	Element	Result (%)
Co	0.02				

X-RAY DIFFRACTION ANALYSIS

CERAC incorporated
P.O. Box 1178, Milwaukee, WI 53201
(414) 289-9800 Phone (414) 289-9805 Fax

Brian T Wegner

Brian T Wegner, QA Engineer *March 4, 2003*

EXPERIMENTAL PROCEDURE FOR NICKEL RUN 14-01-04

EXAMPLE 2

A cylindrical alumina-based crucible (99.68% Al_2O_3, 0.07% SiO_2, 0.08% Fe_2O_3, 0.04% CaO, 0.12% Na_2O_3; 4.5" O.D. x 3.75" I.D. x 10" depth) of a 100 pound induction furnace reactor supplied by Inductotherm, was fitted with a 75-30R Powertrak power supply and charged with 2500 g nickel (99.97% purity) and 100 g of graphite carbon through its charging port. The reactor was fitted with a graphite cap with a ceramic liner (i.e. the crucible, from Engineering Ceramics). During the entire procedure, a slight positive pressure of nitrogen (~0.5 psi) was maintained in the reactor using a continuous backspace purge. The reactor was heated to the metal charge liquidus point, over a rate no greater than 300°F/hour, as limited by the integrity of the crucible. The induction furnace operated in a frequency range of 0 kHz to 3000 kHz, with frequency determined by a temperature-controlled feedback loop implementing an Omega Model CA 300 temperature controller. Upon reaching 2800°F, the reactor was charged with an additional 2700 g nickel over an hour.

The temperature was again increased to 2850°F again using a rate no greater than 300°F/hour. When this temperature was reached, graphite saturation assemblies (3/8" OD, 36" long high purity [<5 ppm impurities] graphite rods) were inserted to the bottom of the nickel charge through ports located in the top plate. The nickel was held at 2850°F for 4 hours. Every 30 minutes during the hold period, an attempt was made to lower the graphite saturation assemblies as dissolution occurred. As the nickel became saturated with carbon, the graphite saturation assemblies were consumed. After the 4 hour hold period was complete, the graphite saturation assemblies were removed.

The reactor temperature was increased to 3256°F over 7 minutes. The temperature was then varied between 2950°F and 3256°F for 15 cycles. Each cycle consisted of lowering the temperature continuously over 7 minutes and raising the temperature continuously over 7 minutes. After the 15 cycles were completed, a gas addition lance was lowered and a 0.15 L/min flow of argon was begun. The temperature of the nickel was varied over another 5 cycles between 2950°F and 3256°F.

After the fifth cycle, the reactor temperature was lowered to 2850°F over a 10 minute period with continued argon addition. The graphite saturation assemblies were reinstalled in the nickel and remained there for 1 hour. The graphite saturation assemblies were removed.

The reactor temperature was lowered to 2829°F over 5 minutes. The reactor was held at this temperature for 5 minutes with continued argon addition. The temperature was then varied between 2790°F and 2829°F over 20 cycles. Each cycle consisted of lowering the temperature continuously over 9 minutes and raising the temperature continuously over 9 minutes. The argon addition ceased after completion of the 20 cycles.

The reactor temperature was lowered to 2770°F over 5 minutes. The temperature was varied between 2710°F and 2770°F over 4 ½ cycles. Each cycle consisted of lowering the temperature continuously over 5 minutes and raising the temperature continuously over 3 minutes. In addition, while raising the temperature, a 0.15 L/min flow of argon was added, and while lowering the temperature, a 0.15 L/min flow of nitrogen was added.

The reactor temperature was lowered to 2691°F over 5 minutes. The temperature was varied between 2492°F and 2691°F for 15.5 cycles. Each cycle consisted of lowering the temperature continuously over 15 minutes and raising the temperature continuously over 15 minutes. In addition, while raising the temperature, a 0.15 L/min flow of argon was added, and while lowering the temperature, a 0.15 L/min flow of nitrogen was added. All gas addition, except for the purge of nitrogen ceased after the 15.5 cycles were completed.

The temperature was varied between 2571°F and 2492°F for one cycle. The cycle consisted of raising the temperature continuously over 15 minutes and lowering the temperature over 15 minutes. The gas addition lance was removed.

The reactor temperature was slowly cooled by lowering the induction furnace power to 1 KW or less as the ingot cooled. The nickel was then cooled to approximately ambient temperature in water.

ANALYTICAL PROTOCOLS

XRF, grain size, magnetism, and chemical reactivity measurements were carried out by the procedures described in Example 1.

ANALYTICAL RESULTS

An x-ray fluorescence analysis of the nickel sample is provided in Figures 28A and 28B, with the K_α and L_α peaks of a nickel control standard shown for reference.

An x-ray fluorescence analysis of the nickel sample is provided in Figure 29A, with the K_α peak of an aluminum control standard shown for reference.

An x-ray fluorescence analysis of the nickel sample is provided in Figure 29B, with the K_α peak of a zirconium control standard shown for reference.

An x-ray fluorescence analysis of the nickel sample is provided in Figure 30A, with the K_α peak of a sulfur control standard shown for reference.

An x-ray fluorescence analysis of the copper sample is provided in Figure 30B, with the K_α peak of an chlorine (from potassium chloride) shown for reference.

Summary data showing the apparent elemental composition of the product of Example 2 is shown in Tables 14-16, as was measured by an XRF analysis using a Uniquant software package. The apparent elemental composition of the product varies by position, which is indicated in each table.

The manufactured nickel retained a large amount of refractory on its exterior surface after retrieval from the reactor. The retained refractory was attributed to either surface attraction or reaction with the high content of Al_2O_3 in the refractory. The ingot did not crack with handling, but did have an internal void. The visible radial surface appeared duller in than the axial (top) face, again demonstrating anisotropic physical properties. The ingot demonstrated no unexpected chemical reactivity after removal from the reaction system.

CERAC™ incorporated
Quality Manufacturing Since 1964

Certificate of Analysis

Item Number	Description	Lot Number
C-1226	COBALT METAL, Co Typically 99.5% pure (excluding Ni) 12 mm shot & smaller	X0030613

SPECIFIC ANALYSIS OR PROPERTY

Test For	Found	Theoretical

SPECTROGRAPHIC ANALYSIS

Element	Found (%)	Element	Found (%)	Element	Found (%)
Fe	0.21	Ni	0.265		

X-RAY DIFFRACTION ANALYSIS

CERAC incorporated
P.O. Box 1178, Milwaukee, WI 53201
(414) 289-9800 Phone (414) 289-9805 Fax

Brian T Wegner

Brian T Wegner, QA Engineer *December 21, 2004*

CERAC Incorporated
PO Box 1178
MILWAUKEE, WI 53201

Telephone .: 414-289-9800
Fax .....: 414-289-9805

Sales Packing slip

Customer Acct # .....: CUS-0 71
Number .....: PAC-016366
Date .....: 12/22/04
Page .....: 1
Sales order .....: SO-264965
Purchase order .....: 20904
Your ref. .....:
Mode of delivery .....: UPS Ground
Terms of delivery .....: FOB Origin
Freight code .....: PrePay & Add
Contact Name .....: Janet Pichette
Contact Phone .....: 508-324-6411
Contact Fax .....:
Contact Email .....:

Sold to : Atomic Ordered Materials, LLC
22 Evergreen Dr.
SEEKONK, MA 02771

Ship to : Atomic Ordered Materials, LLC
421 Currant Road
FALL RIVER, MA 02720

***** Header Comments ****

mk

Item number	Name	Ordered	Delivered	Balance
C-1226	COBALT METAL Co 12 mm shot & smaller Typ. 99.5% (ex Ni) 7440-48-4	20,000.00	20,000.00	

Country of Origin: ZM
COBALT METAL
Quantity : 20,000.00 Warehouse : 1 Batch number : X0030613 Location : 000-0-0
Per Quote 11/04

Schedule B# 8105.20.0000
ECCN # EAR99

Receipt: _____

EXPERIMENTAL PROCEDURE FOR COBALT RUN 14-01-05
EXAMPLE 3

A cylindrical alumina-based crucible (99.68% Al_2O_3, 0.07% SiO_2, 0.08% Fe_2O_3, 0.04% CaO, 0.12% Na_2O_3; 4.5" O.D. x 3.75" I.D. x 10" depth) of a 100 pound induction furnace reactor supplied by Inductotherm and fitted with a 75-30R Powertrak power supply, was charged with 2176 g cobalt (99.8% purity) through its charging port. The reactor was fitted with a graphite cap with a ceramic liner from Engineering Ceramics. During the entire procedure, a slight positive pressure of nitrogen (~0.5 psi) was maintained in the reactor using a continuous backspace purge. The reactor was heated to 2800°F over a minimum of 14 hours while the induction furnace operated in a frequency range of 0 kHz to 3000 kHz. Upon reaching 2700°F, the reactor was charged with an additional 3000 g cobalt over an hour.

When 2800°F was reached, graphite saturation assemblies were inserted to the bottom of the cobalt charge through ports located in the top plate. The cobalt was held at 2800°F for 4 hours. Every 30 minutes during the hold period, an attempt was made to lower the graphite saturation assemblies as dissolution progressed. As the cobalt became saturated with carbon, the graphite saturation assemblies were consumed. After the 4 hour hold period was complete, the graphite saturation assemblies were removed.

The reactor temperature was increased to 3086°F over 7 minutes. The temperature was then varied between 2875°F and 3086°F for 15 cycles. Each cycle consisted of lowering the temperature continuously over 7 minutes and raising the temperature continuously over 7 minutes. After the 15 cycles were completed, a gas addition lance was lowered and a 0.15 L/min flow of argon was begun. The temperature of the cobalt was varied over another 5 cycles between 2875°F and 3086°F.

After the fifth cycle, the reactor temperature was lowered to 2800°F over a 10 minute period with continued argon addition. The graphite saturation assemblies were reinstalled in the cobalt and remained there for 1 hour. The graphite saturation assemblies were removed.

The reactor temperature was lowered to 2785°F over 5 minutes. The reactor was held at this temperature for 5 minutes with continued argon addition. The temperature

was then varied between 2689°F and 2785°F over 20 cycles. Each cycle consisted of lowering the temperature continuously over 9 minutes and raising the temperature continuously over 9 minutes. The argon addition ceased after completion of the 20 cycles.

The reactor temperature was lowered to 2737°F over 5 minutes. The temperature was varied between 2689°F and 2737°F over 4 ½ cycles. Each cycle consisted of lowering the temperature continuously over 5 minutes and raising the temperature continuously over 3 minutes. In addition, while raising the temperature, a 0.15 L/min flow of argon was added, and while lowering the temperature, a 0.15 L/min flow of nitrogen was added.

The reactor temperature was lowered to 2672°F over 5 minutes. The temperature was varied between 2498°F and 2672°F for 15.5 cycles. Each cycle consisted of lowering the temperature continuously over 15 minutes and raising the temperature continuously over 15 minutes. In addition, while raising the temperature, a 0.15 L/min flow of argon was added, and while lowering the temperature, a 0.15 L/min flow of nitrogen was added. All gas addition, except for the purge of nitrogen ceased after the 15.5 cycles were completed.

The temperature was varied between 2570°F and 2498°F for one cycle. The cycle consisted of raising the temperature continuously over 15 minutes and lowering the temperature continuously over 15 minutes. The gas addition lance was removed.

The reactor temperature was cooled by lowering the induction furnace power to 1 kW or less as the ingot cooled. The cobalt was then cooled to approximately ambient temperature in water.

ANALYTICAL PROTOCOLS

XRF, grain size, magnetism, and chemical reactivity measurements were carried out by the procedures described in Example 1.

ANALYTICAL RESULTS

An x-ray fluorescence analysis of the cobalt sample is provided in Figures 31A and 31B, with the K_α and L_α peaks of a cobalt control standard shown for reference.

An x-ray fluorescence analysis of the cobalt sample is provided in Figure 32A, with the K_α peak of an aluminum control standard shown for reference.

An x-ray fluorescence analysis of the cobalt sample is provided in Figure 32B, with the K_α peak of an iron control standard shown for reference.

An x-ray fluorescence analysis of the cobalt sample is provided in Figure 33A, with the K_α peak of a chlorine (from potassium chloride) control standard shown for reference.

An x-ray fluorescence analysis of the cobalt sample is provided in Figure 33B, with the K_α peak of a zirconium control standard shown for reference.

An x-ray fluorescence analysis of the cobalt sample is provided in Figure 34, with the K_α peak of a manganese control standard shown for reference.

Summary data showing the apparent elemental composition of the product of Example 3 is shown in Table 17, as was measured by an XRF analysis using a Uniquant software package.

The top (axial) face of the manufactured cobalt ingot exhibited many of the recursive patterns observed in other manufactured ingots. The surface peaks are inconsistent with what would be expected given the forces of gravity during cooling. In addition, the shiny top face of the ingot exhibited an unexpected coloration, such that some of the faces had a distinct pink tint. While the top of the ingot was shiny, silver metallic, the sides of the ingot were matte silver in appearance.

The manufactured cobalt ingot retained a small amount of refractory around its base. The ingot did not crack upon retrieval from the reaction system. No unexpected magnetic behavior or chemical reactivity were observed.

Compare al		Drop all "<" data		11/15/2005		10/24/2005		11/21/2005		1/6/2006			1/6/2006		
		GDMS		GDMS		XRF-UWO		PIXE		GDOES			GDOES		
		Al chunks		Aluminum		Aluminum		Aluminum		5 ppm OEM Limit			5 ppm OEM Limit		
				14-01-10		14-01-10		14-01-10		Aluminum			Aluminum		
		Average	Max	Al B (99.9%wt)		Al B (99.9%wt)		Al B (99.9%wt)		14-01-10A			14-01-10R		
			99.9999	axial	radial	axial	radial	axial	radial	Al B (99.9%wt)			Al B (99.9%wt)		
1	H									40-45	Ave 0.05-15	Ave 15-100	40-45	Ave 0.05-15	Ave 15-130
2	He														
3	Li														
4	Be														
5	B	0.05	#DIV/0!							118	108.9	110.5	100.7	100.6	100.3
6	C				25						1612			501.4	
7	N										364.2			101.7	
8	O			110	220			180540	434010	7418	32100	7869	6722	12260	8351
9	F														
10	Ne														
11	Na	0.17666667	0.2442188				470								
12	Mg	14.3333333	17.7109299												
13	Al					986300	961900	837250	558740	983400	950400	982800	983400	972900	982300
14	Si	21.0666667	28.4218597	770	560	9400	31800			531.3	1985	815.2	1341	1286	1422
15	P	0.49666667	0.64388269								22.78			57.49	
16	S	0.29666667	0.43554849						767.097	103.1	305.8	107.8	98.82	297	101.2
17	Cl	0.075	0.20165987			253	811		1100						
18	Ar														
19	K														
20	Ca	0.5	#DIV/0!			84	186		253.583	150.1	218.8	146.7	135.8	175	135.9
21	Sc	0.02666667	0.04355465												
22	Ti	0.41	0.88885895			790	1460	390.911	1550		315.6				
23	V	0.16333333	0.25269614		31					112.9	23.43	124.9	131.7	87.76	150.3
24	Cr	0.29666667	0.44389269				74			61.4	75.91	62.13	58.27	59.2	59.61
25	Mn	0.10333333	0.1371093												
26	Fe	14.3333333	17.7109299	770	790	2230	1950	1270	1720	1117	1087	1091	1598	2061	1887
27	Co	0.05666667	0.17488255						48.222	440.3	484.4	442.1	410.3	431.6	420.6
28	Ni	0.28333333	0.83704287	34	30	81	79	43.972	66.127						
29	Cu	13.0666667	17.0442632	26		387	583	373.198	1520		1228			1500	
30	Zn	1.96666667	3.18447842					21.729	32.678		827.1			440.9	
31	Ga	0.29666667	0.44389269	57	50	89	97	64.458	58.375						
32	Ge														
33	As									2682	2583	2792	2671	2996	2900
34	Se														
35	Br														
36	Kr														
37	Rb														
38	Sr														
39	Y	0.025	0.05033197												
40	Zr	0.12333333	0.21269614					22.714	58.605	57.85		77.17	70.33	45.52	105.8
41	Nb											31.67	40.08	28.99	75.99
42	Mo	0.06333333	0.0971093												
43	Tc														
44	Ru														
45	Rh														
46	Pd														
47	Ag														
48	Cd													20.89	
49	In														
50	Sn									279.7	859.4	278.6	259.3	579.5	267.2
51	Sb									3113	2987	3192	3079	3269	3344
52	Te														
53	I														
54	Xe														
55	Cs														
56	Ba	0.15666667	0.45687401												
57	La	0.33	1.00467438												
58	Ce	0.42333333	1.33403258												
59	Pr	0.11666667	0.35309842												
60	Nd	0.32333333	1.17580018												
61	Pm														
62	Sm														
63	Eu						52								
64	Gd	0.09	#DIV/0!												
65	Tb														
66	Dy														
67	Ho														
68	Er	0.02	#DIV/0!												
69	Tm														
70	Yb														
71	Lu														
72	Hf														
73	Ta														
74	W	0.26666667	0.87557184												
75	Re														
76	Os														
77	Ir														
78	Pt														
79	Au														
80	Hg														
81	Tl														
82	Pb	0.06	0.11066395								68.05			46.43	
83	Bi									375.6	1284	382.1	317	671.5	320.6
84	Po														
85	At														
86	Rn														
87	Fr														
88	Ra														
89	Ac														
90	Th	0.09	0.1913379												
91	Pa														
92	U	[illegible]	[illegible]												
						82.1644	83.7044	13.824	64.656			66.30			129.80
												0.1			0.1

Compare at				10/28/2005				10/24/2005		11/21/2005		1/6/7			1/6/2006		
		GDMS		GDMS				XRF-UWO		PIXE		GD			GDOES		
		Confidence Interval										5 ppm OEM Limit			5 ppm OEM Limit		
		Cu Chop		Copper				Copper		Copper		Copper			Copper		
				14-00-01				14-00-01		14-00-01		14-00-01A			14-00-01R		
				Patent				Patent		Patent		Patent			Patent		
		Average	Max														
No			99.9999	axial		radial		axial	radial	axial	radial	40-45	Ave 0.05-15	Ave 15-155	40-45	Ave 0.05-15	Ave 15-115
1	H																
2	He																
3	Li																
4	Be																
5	B	0.0010	#DIV/0!														
6	C												63.25			56.12	
7	N																
8	O									235250	128860	1683	3290	1534	634.3	3142	678.9
9	F																
10	Ne																
11	Na																
12	Mg	0.0040	0.0125									288.6	314	251.7	241.4	249	231.7
13	Al	0.3938	2.3019					1350		959.198	1910	50.15	255.6	31.71		126.6	
14	Si	0.0760	0.1689					6530	5640	1400	6320						
15	P	0.0130	0.0485									1823	1450	2105	2435	2158	2598
16	S	3.6600	8.3912	24		24						20.7	40.23	20.47	22.01	45.08	23.01
17	Cl	0.1260	0.2146					112	182	350.719	212.406						
18	Ar																
19	K	0.0300	#DIV/0!														
20	Ca											20.75	24.22				
21	Sc																
22	Ti	0.0114	0.0302						53								
23	V																
24	Cr	0.0340	0.1657														
25	Mn	0.0136	0.0391														
26	Fe	2.1520	4.8122					53		472.395	461.03	62.38	73.99	57.38	53.6	61.79	52.49
27	Co	0.0140	0.0382									56.66	56.74	52.08	40.65	37.93	40.97
28	Ni	0.5529	1.0635														
29	Cu			Matrix		Matrix		991100	993300	761580	862230	995600	993900	995500	996100	993500	995900
30	Zn																
31	Ga																
32	Ge																
33	As	0.4760	0.6351														
34	Se	0.6160	0.9602														
35	Br																
36	Kr																
37	Rb																
38	Sr																
39	Y																
40	Zr																
41	Nb																
42	Mo	0.0153	0.0390														
43	Tc																
44	Ru																
45	Rh							372	315								
46	Pd																
47	Ag	8.7800	10.2431									42.7	43.75	40.91	42.83	43.48	42.11
48	Cd																
49	In																
50	Sn	0.2900	0.7513									113.7	141.1	116.3	126.1	166.7	126.8
51	Sb	0.4960	1.1273														
52	Te	0.1340	0.3199									71.09	45.64	87.97	97.42	91.3	106.8
53	I																
54	Xe																
55	Cs																
56	Ba	0.0035	0.0060														
57	La								105								
58	Ce																
59	Pr																
60	Nd																
61	Pm																
62	Sm																
63	Eu																
64	Gd																
65	Tb																
66	Dy																
67	Ho																
68	Er																
69	Tm																
70	Yb								149								
71	Lu																
72	Hf																
73	Ta																
74	W	0.2183	1.1874														
75	Re							126	155								
76	Os																
77	Ir							116	76								
78	Pt																
79	Au																
80	Hg																
81	Tl																
82	Pb	0.7820	1.0283									91.85	83.3	85.1	109.5	104	109.5
83	Bi	0.1219	0.2722									57.63	116.1	61.99	89.71	147.8	84.49
84	Po																
85	At																
86	Rn																
87	Fr																
88	Ra																
89	Ac																
90	Th																
91	Pa																
92	U																
								99.00%	100.30%	78.475	87.114			200.00			110.30
														NA			0.2

Compare at		GDMS	7/10/2006	7/14/2006 GDMS		7/17/2006 PIXE		5/24/2001 XRF-ADM		12/10/2005 NAA	
		Confidence Interval								20-31%	20-22%
		SI Powder	Silicon 14-06-05	Silicon 15-01-01		Silicon 15-01-01 Patent		Silicon 15-01-01		Silicon 15-01-01	
		Average	Max	Starting Material n/a							
			99.9999		axial	radial	axial	radial	axial	radial	axial	radial
1	H											
2	He											
3	Li											
4	Be											
5	B											
6	C											
7	N											
8	O						67450	30830				
9	F											
10	Ne											
11	Na	0.3800	0.6789						40	180		
12	Mg	0.2000										
13	Al	0.7367	0.8173		2000	3400	16650	21400	11800	14800		
14	Si						912030	941180	965800	981200	934000	954000
15	P				32	56			130	180		
16	S	0.2500	0.4708				1360	3110	130			
17	Cl	3.6667	7.0443						40	190		
18	Ar								130	120		
19	K									140		
20	Ca						5780	2100	92	770		
21	Sc											
22	Ti	0.0867	0.2983		38	78	550.759	526.661	190	290		
23	V											
24	Cr	2.4667	5.4667				22.098		31	26		
25	Mn	0.8333	1.0596									
26	Fe	81.3333	82.8945	60	130	190	814.655	502.431	550	420		300
27	Co	0.0833	0.1080					31.71				
28	Ni	0.8267	1.3896				108.792	31.319	51	53		
29	Cu	0.1900	0.2193		30	52	280.979	145.983	120	101		122
30	Zn						59.206	71.41	21			
31	Ga					22	31.998	31.419	38	43		22.5
32	Ge											
33	As											
34	Se											
35	Br											
36	Kr											
37	Rb											
38	Sr											
39	Y											
40	Zr											
41	Nb											
42	Mo	0.0800										
43	Tc											
44	Ru											
45	Rh											
46	Pd											
47	Ag											
48	Cd											
49	In											
50	Sn											
51	Sb											
52	Te											
53	I											
54	Xe											
55	Cs											
56	Ba								80			
57	La											
58	Ce											
59	Pr											
60	Nd											
61	Pm											
62	Sm											
63	Eu											
64	Gd											
65	Tb											
66	Dy											
67	Ho											
68	Er											
69	Tm											
70	Yb											
71	Lu											
72	Hf											
73	Ta									30		
74	W	0.3700	0.8029									
75	Re								70	110		
76	Os											
77	Ir											
78	Pt											
79	Au											
80	Hg											
81	Tl											
82	Pb											
83	Bi	0.6200					39.867	24.08				
84	Po											
85	At											
86	Rn											
87	Fr											
88	Ra											
89	Ac											
90	Th											
91	Pa											
92	U											
							93.755	96.917	83.40%	79.70%		

Compare at	Date	7/10/2006	7/14/2006		7/17/2006		8/1/2001	
Zn	analysis	GDMS	GDMS		PIXE		XRF-ADM	
	electrical							
type	conductivity type	Iron	Iron		Iron		Iron	
	origin	Starting Material	15-01-02		15-01-02		15-01-02	
	comment	n/a			Patent			
No			axial	radial	axial	radial	axial	radial
1	H							
2	He							
3	Li							
4	Be							
5	B							
6	C							
7	N							
8	O				86800	22510		
9	F							
10	Ne							
11	Na							400
12	Mg							
13	Al		5100	6200	10060	20240	18900	29600
14	Si		460	460	1370	2340	320	1400
15	P		52	31			33	36
16	S		37	23		281.985		
17	Cl						40	44
18	Ar						120	130
19	K							
20	Ca					193.727	53	73
21	Sc						25	26
22	Ti							
23	V							
24	Cr		21					
25	Mn							
26	Fe				901980	954430	980100	967800
27	Co			21				
28	Ni		44	36				
29	Cu						120	140
30	Zn							
31	Ga							
32	Ge							
33	As							
34	Se							
35	Br							
36	Kr							
37	Rb							
38	Sr							
39	Y							
40	Zr		160	110			99	120
41	Nb							
42	Mo							
43	Tc							
44	Ru							
45	Rh							
46	Pd							
47	Ag							
48	Cd							
49	In							
50	Sn							
51	Sb							
52	Te							
53	I							
54	Xe							
55	Cs							
56	Ba							
57	La							
58	Ce							
59	Pr							
60	Nd							
61	Pm							
62	Sm							
63	Eu							
64	Gd							
65	Tb							
66	Dy							
67	Ho							
68	Er							
69	Tm							
70	Yb							
71	Lu							
72	Hf							
73	Ta							
74	W						90	
75	Re							
76	Os							
77	Ir							
78	Pt							
79	Au							
80	Hg							
81	Tl							
82	Pb							
83	Bi							
84	Po							
85	At							
86	Rn							
87	Fr							
88	Ra							
89	Ac							
90	Th						80	
91	Pa							
92	U							
					81.34	97.749	98.80%	97.80%

Compare el		7/10/2006	[illegible]/2006		7/17/2006		6/1/2001	
[illegible]	analysis	GDMS	[illegible]S		PIXE		XRF-AOM	
	[illegible]							
[illegible]	sample type	Cobalt	Cobalt		Cobalt		Cobalt	
	weight	Starting Material	14-01-05		14-01-05		14-01-05	
	[illegible]	n/a			Patent			
			axial	radial	axial	radial	axial	radial
1	H							
2	He							
3	Li							
4	Be							
5	B							
6	C							
7	N							
8	O					70470		
9	F							
10	Ne							
11	Na						260	430
12	Mg							
13	Al	500	5000	3500	33280	16800	49000	37100
14	Si	55	650	800	3480	1980	730	1800
15	P			25			40	37
16	S	47	50	150	730.378	527.381		
17	Cl				748.054		47	34
18	Ar						110	100
19	K							
20	Ca				381.592	201.684	75	87
21	Sc						22	33
22	Ti							
23	V							
24	Cr							
25	Mn	50	50	50			91	81
26	Fe		1000	1000	1550	1690	1300	1300
27	Co				959830	908330	948000	957000
28	Ni		1500	1500			1600	1800
29	Cu	120	130	130				
30	Zn	50						
31	Ga							
32	Ge							
33	As							
34	Se							
35	Br							
36	Kr							
37	Rb							
38	Sr							
39	Y							
40	Zr		100	200			190	170
41	Nb			130				
42	Mo		25	50				
43	Tc							
44	Ru							
45	Rh							
46	Pd							
47	Ag							
48	Cd						30	
49	In							
50	Sn							
51	Sb							
52	Te							
53	I							
54	Xe							
55	Cs							
56	Ba						80	
57	La							
58	Ce							
59	Pr							
60	Nd							
61	Pm							
62	Sm							
63	Eu							80
64	Gd						100	110
65	Tb							
66	Dy							
67	Ho							
68	Er							
69	Tm							
70	Yb							
71	Lu							
72	Hf						140	
73	Ta							
74	W			50				
75	Re							
76	Os							
77	Ir							
78	Pt							
79	Au							
80	Hg							
81	Tl							
82	Pb							
83	Bi							
84	Po							
85	At							
86	Rn							
87	Fr							
88	Ra							
89	Ac							
90	Th							
91	Pa							
92	U							
					69.833	67.833	191.85%	191.85%

Compare at		7/10/2006	7/24/2006		7/17/2006		5/24/2001	
		ODM3	ODM3		PIXE		XRF-AOM	
		Nickel Starting Material n/a	Nickel 14-01-04		Nickel 14-01-04 Patent		Nickel 14-01-04	
			axial	radial	axial	radial	axial	radial
1	H							
2	He							
3	Li							
4	Be							
5	B							
6	C							
7	N							
8	O				80850	30420		
9	F							
10	Ne							
11	Na						310	1200
12	Mg							
13	Al				17520	19470	21100	25700
14	Si		190	250	516.734	868.145	300	1400
15	P							
16	S							
17	Cl							50
18	Ar							100
19	K							48
20	Ca					790.087		110
21	Sc						24	
22	Ti							
23	V							
24	Cr							
25	Mn							
26	Fe		34	39		240.679		
27	Co							
28	Ni				921120	948200	971000	984300
29	Cu							
30	Zn							
31	Ga							
32	Ge							50
33	As							
34	Se							
35	Br							
36	Kr							
37	Rb							
38	Sr							
39	Y							
40	Zr		240	250			270	320
41	Nb							
42	Mo							
43	Tc							
44	Ru							
45	Rh						50	
46	Pd							
47	Ag							
48	Cd							
49	In							
50	Sn							
51	Sb							
52	Te							
53	I							
54	Xe							
55	Cs							
56	Ba							60
57	La							
58	Ce							
59	Pr							
60	Nd							
61	Pm							
62	Sm							
63	Eu							
64	Gd							
65	Tb							
66	Dy							
67	Ho							
68	Er							
69	Tm							
70	Yb							
71	Lu						8800	9400
72	Hf							
73	Ta							
74	W							
75	Re							
76	Os							
77	Ir							
78	Pt							
79	Au							
80	Hg							
81	Tl							
82	Pb							
83	Bi							
84	Po							
85	At							
86	Rn							
87	Fr							
88	Ra							
89	Ac							
90	Th							
91	Pa							
92	U							
					F3.618	94.858	101.40%	100.80%

This Page is Inserted by IFW Indexing and Scanning Operations and is not part of the Official Record

BEST AVAILABLE IMAGES

Defective images within this document are accurate representations of the original documents submitted by the applicant.

Defects in the images include but are not limited to the items checked:

- ☐ BLACK BORDERS
- ☐ IMAGE CUT OFF AT TOP, BOTTOM OR SIDES
- ☐ FADED TEXT OR DRAWING
- ☐ BLURRED OR ILLEGIBLE TEXT OR DRAWING
- ☐ SKEWED/SLANTED IMAGES
- ☑ COLOR OR BLACK AND WHITE PHOTOGRAPHS
- ☐ GRAY SCALE DOCUMENTS
- ☑ LINES OR MARKS ON ORIGINAL DOCUMENT
- ☐ REFERENCE(S) OR EXHIBIT(S) SUBMITTED ARE POOR QUALITY
- ☐ OTHER: _____

IMAGES ARE BEST AVAILABLE COPY.
As rescanning these documents will not correct the image problems checked, please do not report these problems to the IFW Image Problem Mailbox.